Please cite this article in press as: Argudo and Purohit, Competition between Supercoils and Toroids in Single Molecule DNA Condensation, Biophysical Journal (2012), doi:10.1016/j.bpj.2012.05.033

Competition between Supercoils and Toroids in Single Molecule DNA Condensation

David Argudo and Prashant K. Purohit*
Department of Mechanical Engineering and Applied Mechanics, University of Pennsylvania, Philadelphia, Pennsylvania

ABSTRACT The condensation of free DNA into toroidal structures in the presence of multivalent ions and polypeptides is well known. Recent single molecule experiments have shown that condensation into toroids occurs even when the DNA molecule is subjected to tensile forces. Here we show that the combined tension and torsion of DNA in the presence of condensing agents dramatically modifies this picture by introducing supercoiled DNA as a competing structure in addition to toroids. We combine a fluctuating elastic rod model of DNA with phenomenological models for DNA interaction in the presence of condensing agents to compute the minimum energy configuration for given tension and end-rotations. We show that for each tension there is a critical number of end-rotations above which the supercoiled solution is preferred and below which toroids are the preferred state. Our results closely match recent extension rotation experiments on DNA in the presence of spermine and other condensing agents. Motivated by this, we construct a phase diagram for the preferred DNA states as a function of tension and applied end-rotations and identify a region where new experiments or simulations are needed to determine the preferred state.

INTRODUCTION

Several experimental studies on DNA aggregation and condensation (1–6) have been carried out under a wide range of salt concentrations because of its physiological relevance, especially during the cell cycle (7,8). The counterion-induced condensation of DNA is reproduced without difficulty in experiments and yet it is still not fully understood although it is a fundamental and crucial process for our very existence (9). Multivalent ions promote DNA bending because they neutralize the negative charges on DNA phosphate, which facilitates enhanced protein-DNA interaction, and they may play an important role in facilitating transcription (7). Protamine-DNA assemblies closely resemble those of DNA condensed by multivalent ions that have less charge and are much smaller in size (10). Protamine binds and condenses DNA into compact configurations in the sperm of most vertebrates; it inactivates and packages centimeters of DNA in the sperm head (size of a micron approximately) until DNA is reactivated after fertilization (9).

In this study, to gain a deeper understanding of more complex forms of DNA packing, we extend the results obtained in Argudo and Purohit (11) to make predictions for DNA single-molecule experiments in the presence of high concentration of condensing agents and low concentration of monovalent salt.

Most DNA condensation experiments at high multivalent ionic concentrations have been focused on free molecules in bulk solution (12–15), where toroidal structures have been observed. In addition to the experiments in bulk, the force-extension curves in single-molecule experiments under controlled force/extension in high multivalent ionic solutions have been measured (6,16). It has been demonstrated that DNA is incorporated into the collapsed condensate in discrete steps (6,17–19) and it has been seen that DNA condenses into a single collapsed structure (torus) (18). More sophisticated single-molecule experiments have recently been performed by Besteman et al. (5) in which DNA molecules in high multivalent salt solutions were subjected to an applied tension and end-rotations. They suggested a simple model to explain their experimental findings, proposing the idea that the DNA compaction starts with the formation of a loop. But it is still not clear what would be the final compact DNA structure (toroids or supercoils) in the presence of high concentrations of multivalent ions under imposed end-rotations. Through our model, we can provide an answer to this question by mapping the different DNA states in a phase diagram constructed by computing and comparing the energies of each state as a function of the external force and number of turns.

We have used a variational approach to solve a constrained energy-minimization problem that corresponds to angular optical-trap (or magnetic-tweezers) experiments on a DNA molecule attached to a substrate at one end while subjected to a tensile force and twisted by a specific number of turns n at the other end in the presence of condensing agents (see Fig. 1). Our model is valid in the overtwisting regime only for moderately large values of n (before a structural transition into P-DNA (20)), where the results of Moroz and Nelson (21) for the entropic elasticity of a twisted polymer are also valid and the DNA can be modeled with constant elastic properties along the entire molecule. In our one-dimensional continuum description of the DNA molecule, we account for DNA elasticity, DNA-DNA interactions, fluctuations, and configurational entropy in the tails,

Submitted February 23, 2012, and accepted for publication May 21, 2012.

*Correspondence: purohit@seas.upenn.edu

Editor: Laura Finzi.

0006-3495/12/07/0001/11 $2.00

doi: 10.1016/j.bpj.2012.05.033

Please cite this article in press as: Argudo and Purohit, Competition between Supercoils and Toroids in Single Molecule DNA Condensation, Biophysical Journal (2012), doi:10.1016/j.bpj.2012.05.033

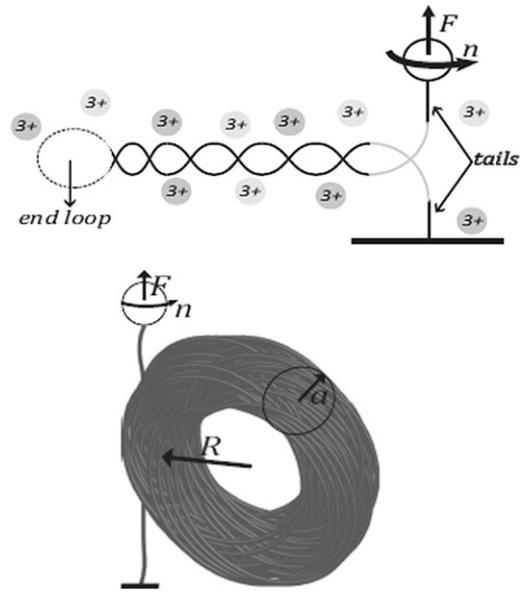

FIGURE 1 Multivalent ions with three or more positive charges can cause condensation. In a given experiment only one type of ion is typically used. The DNA molecule is fixed at one end, whereas the other end is subjected to a pulling force F and twisted by n number of turns. (*Top*) Sketch representing the formation of supercoiled structure in single-molecule experiments in the presence of condensing agents. (*Bottom*) Sketch representing the formation of a toroid.

helices, and toroidal loops. For the description of the toroidal structures, we have added the twist effects to a well-established model (22,23). And for the description of the supercoiled structures, we follow the treatment in Argudo and Purohit (11) including the effects of multivalent cations in the internal energy.

DNA SUPERCOILING

In this section, we study supercoils. We describe the straight-supercoiled configuration of the DNA, which corresponds to the coexistence of a helical region (plectonemes) and straight portions of the DNA molecule (tails). The analysis of the transition from the straight configuration into the straight-supercoiled configuration is known to be a dynamic process (24–26) and a simplified analysis based on equilibrium energetics (11) will be done in DNA Transitions and Formation of Supercoils. But first, we briefly describe the DNA straight configuration before the supercoiling transition and the straight-supercoiled configuration after the transition.

Straight configuration

As shown in Argudo and Purohit (11), the energy of the straight state under imposed end-rotations and tension is given by a Legendre transform of the energy under controlled torque given by Moroz and Nelson (21),

$$V_s = \left(\frac{M^2}{2K_t} + G^*_{flu} + \frac{M^2}{4K_bK} - F\right)L, \tag{1}$$

where F is the external force applied, M is the external moment in the straight configuration due to the end-rotations,

$$K = \frac{\sqrt{K_bF - M^2/4}}{k_BT}, \tag{2}$$

and the term G^*_{flu} is a correction to the energy due to thermal fluctuations (21),

$$G^*_{flu} = \frac{(k_BT)^2}{K_b}K\left(1 - \frac{1}{4K} - \frac{1}{64K^2}\right) + O\left(K^{-3}\right), \tag{3}$$

where k_B is the Boltzmann constant and T is the absolute temperature. The bending modulus of the DNA filament is denoted by K_b and the twisting modulus is denoted by K_t.

The external torque M in the straight configuration can be obtained from the imposed number of turns n_{c-s}, which is equal to the linking number of the DNA molecule (21). The link corresponds to the classical partition into twist and writhe (27,28). The contribution of the thermal fluctuations to the total writhe can be accounted for by using the results of Moroz and Nelson (21):

$$n_{c-s} = \frac{M}{2\pi}\left(\frac{1}{K_t} + \frac{1}{4K_bK}\right)L + O\left(K^{-3}\right). \tag{4}$$

Straight-supercoiled configuration

In the straight-supercoiled state, we will model DNA as consisting of three distinct regions: tails, helices, and end-loop. The helical region is characterized by the helical radius r and angle θ, which are assumed to be uniform. This assumption has been previously used in several theoretical studies of plectonemes (29–32) giving results agreeing with experiment.

The molecule contour length spent in the tail is denoted l_t, the end-loop length is denoted l_o, and the contour length in the helices is denoted l_p. The sum of the length of all regions is equal to the total length of the DNA chain L. The equilibrium configuration of the rod is fully specified by the centerline, through the variables r, θ and the external moment in the presence of supercoils $M_3 \neq M$ (11). In what follows we compute these parameters as functions of the loading (pulling force F and the number of turns n) by minimizing the total energy of the system.

The experiments are performed under imposed end-rotations, therefore the energy minimization will be performed under the constraint that the number of turns n imposed

Please cite this article in press as: Argudo and Purohit, Competition between Supercoils and Toroids in Single Molecule DNA Condensation, Biophysical Journal (2012), doi:10.1016/j.bpj.2012.05.033

on the bead is equal to the excess link Lk of the DNA molecule in the tails, helices, and end-loop (11),

$$n_{c-p} = Lk_p + Lk_t + Lk_o, \tag{5}$$

where Lk_p is the link in the helical regime,

$$Lk_p = \frac{M_3 l_p}{2\pi K_t} - \chi \frac{\sin 2\theta}{4\pi r} l_p, \tag{6}$$

and where χ stands for the chirality of the helix (29). Note that rotations n inducing a positive external moment M_3 generate a left-handed helix $\chi = -1$, whereas a right-handed helix $= 1$ corresponds to negative external moments. The contribution of the tails to the total link of the straight-supercoiled configuration is given by Eq. 4 replacing the total DNA length L with the tail's length $l_t - L = l_p - l_o$,

$$Lk_t = \frac{M_3 l_t}{2\pi}\left(\frac{1}{K_t} + \frac{1}{4K_b K_3}\right) + O\left(K^{-3}\right), \tag{7}$$

where K_3 is given by Eq. 2 replacing M with M_3. The link in the end-loop can be approximated as done in Argudo and Purohit (11),

$$Lk_o \approx \frac{M_3 l_o}{2\pi K_t} + 1, \tag{8}$$

where $l_o \approx 4\sqrt{K_b/F}$ (homoclinic loop (33)) and we have used the approximation that the writhe present in the end-loop is equal to 1.

An approximation of the potential energy in the straight-supercoiled configuration can be written by separating the terms that contribute along L, l_p, and l_o (11),

$$\begin{aligned} V_{p-s} = &\left(K_b \frac{\sin^4\theta}{2r^2} + F + U(r,\theta) - G_3^* - \frac{M_3^2}{4K_b K_3}\right) l_p \\ &+ \left(\frac{M_3^2}{2K_t} - F + G_3^* + \frac{M_3^2}{4K_b K_3}\right) L \\ &+ \left(2F - G_3^* - \frac{M_3^2}{4K_b K_3}\right) l_o \\ &+ \nu\left(n - Lk_p - Lk_t - Lk_o\right), \end{aligned} \tag{9}$$

where we have introduced the constraint from Eq. 5 via the Lagrange multiplier ν. The term G_3^* is the correction to the energy due to thermal fluctuations (21) and is given by Eq. 3 with K_3 (evaluated with M_3 instead of M) replacing K. The term $U(r,\theta)$ in the set of energy expressions in Eq. 9 describes the internal energy interactions in the helical regime and it will depend on the type of ions that dominate the salt solution. The appropriate interaction model for multivalent ions will be described in the next sections.

Minimization of the energy (Eq. 9), with respect to the unknown variables l_p, r, θ, and M_3, yields

$$\nu = 2\pi M_3 + O\left(K^{-3}\right), \tag{10}$$

$$\frac{K_b \sin^4\theta}{r^3} - \frac{\partial U(r,\theta)}{\partial r} = -\chi M_3 \frac{\sin 2\theta}{2r^2}, \tag{11}$$

$$K_b \frac{2\sin^3\theta\cos\theta}{r^2} + \frac{\partial U(r,\theta)}{\partial \theta} = -\chi M_3 \left(\frac{\cos 2\theta}{r}\right), \tag{12}$$

$$K_b \frac{\sin^4\theta}{2r^2} + U(r,\theta) + F - G_3^* = -\chi \frac{M_3 \sin 2\theta}{2r}. \tag{13}$$

The system of equations above gives the solution to the variables r, θ, and M_3 that describe the energy per unit length in the straight-supercoiled configuration as a function of the applied force F.

Interaction energy in high multivalent salt

When multivalent ions dominate the solution, the electrostatic potential is known to be repulsive-attractive (2).

We assume that the electrostatic interaction between the helices is approximately equal to the interaction between DNA strands in a hexagonal array. The validity of our assumption will have to be borne out of the comparison with experimental data. It was certainly adequate for studying forces during DNA packing in viruses (34,35). Therefore, we prescribe the electrostatic contribution $U_{es}(r,\theta) \approx U_{es}(r)$, where $U_{es}(r)$ is obtained by relating the osmotic pressure to the total energy of a hexagonal array of parallel DNA filaments (2,36). In the repulsive-attractive regime, Todd et al. (36) propose a phenomenological model for the total pressure between the two DNA strands,

$$\Pi = -C_A \exp\left(-\frac{D}{\lambda}\right) + C_R \exp\left(-\frac{2D}{\lambda}\right), \tag{14}$$

where $D = 2r$ is equal to the spacing between the strands, and $\lambda \approx 4.8 \pm 0.5$ Å is the characteristic decay length. The parameters C_A and C_R describe the attractive and repulsive interactions, respectively. As stated in Todd et al. (36), at the equilibrium spacing $D = D_{eq}$ the attractive and repulsive forces are equal such that $\Pi = 0$, and consequently $C_R = C_A \exp(D_{eq}/\lambda)$. The electrostatic potential per unit length is given by Todd et al. (36) as

$$\begin{aligned} U_{es}(r) &= -\int_{\infty}^{2r} \sqrt{3}\Pi D\, dD \\ &= \frac{\sqrt{3}\lambda}{e^{4r/\lambda}}\left[\frac{C_R}{4}(4r+\lambda) - C_A(2r+\lambda)e^{2r/\lambda}\right]. \end{aligned} \tag{15}$$

Please cite this article in press as: Argudo and Purohit, Competition between Supercoils and Toroids in Single Molecule DNA Condensation, Biophysical Journal (2012), doi:10.1016/j.bpj.2012.05.033

The equilibrium spacing D_{eq} for some condensing agents has been measured experimentally and is $D_{eq} \approx 2.8$ nm (36). The factor of $\sqrt{3}$ enters because each DNA strand is surrounded by six others in a hexagonal array.

The total internal energy is the result of adding the effects of the electrostatic potential U_{es} and the cost of configurational entropy $U_{conf\text{-}helix}$. The free energy of entropic confinement per unit-length of the strand in the plectonemic supercoil is given by (37,38)

$$U_{conf-helix} = \frac{k_B T}{A^{1/3}} \left[\frac{c_p}{(p\pi)^{2/3}} + \frac{c_r}{r^{2/3}} \right], \qquad (16)$$

where $A = K_b/(k_B T)$ is the persistence length of the DNA chain. The terms c_r and c_p are, in general, unknown constants fitted to experiment (38). In our calculations, we will use the terms $c_r = c_p = 2^{-8/3}$, which are empirically optimized constants as given by van der Maarel (38). The term $2\pi p$ is the pitch of the helix and is given by $p = r\cot\theta$. In the expression given for $U_{conf\text{-}helix}$, we assume that the undulations in the radial direction of the helix are not restrained by electrostatics but only by the structure of the plectoneme. When using $c_r = c_p = 2^{-8/3}$, the free energy of entropic confinement per unit-length is small compared to the mechanical and electrostatic energetic contributions. So, small errors in the values of c_r and c_p can be subsumed into the value of C_A, which we treat as a fitting parameter.

Solution for the superhelix parameters

Using $U(r,\theta) = U_{es} + U_{conf\text{–}helix}$ with C_A and D_{eq} values found in the hexagonal array experiments of Todd et al. (36), it is interesting to find that the system of equations found in Eqs. 11–13 has a nontrivial solution only for forces larger than a threshold force F_T. Table 1 summarizes the qualitative effects of the bending modulus K_b and the electrostatic parameters (C_A, D_{eq}) on the supercoiling variables and the slope of the hat curves, as a function of the applied force F.

In Fig. S1 in the Supporting Material we present a more detailed analysis of the effects of the parameters K_b, C_A, and D_{eq} on the supercoiling variables. As a general trend, the helical radius r is approximately constant and close to $D_{eq}/2$. As $F \to F_T$, the slope increases sharply, $2r \to D_{eq}$, and the values of M_3 and θ decrease, which means that the helices are getting less tight (see Fig. S1). The solution to the system of equations found in Eqs. 11–13 shows that the equilibrium values of θ and M_3 approach a positive nonzero value as $F \to F_T$ because of the direct dependence of the internal energy U on $(\cot\theta)^{-2/3}$.

In the next section, we will analyze the DNA phase-transition into supercoiled structures.

TABLE 1 K_b, C_A, and D_{eq} effects

Parameter	F_T	M_3	θ	r	$d\Delta z/dn$
$C_A \uparrow$	↑	↓	↓	↑	↑
$K_b \uparrow$	↓	↑	↓	—	↑
$D_{eq} \uparrow$	↓	↑	↑	↑	↓

A variable's increase and decrease are denoted by ↑ and ↓, respectively. Long-dash means no significant effect.

DNA transitions and formation of supercoils

When multivalent ions dominate the solution, the results from the transition have some similar features to the ones found for monovalent ions including the possibility of a transition straight → straight-supercoil and the transition straight-supercoil → pure plectoneme (for sufficiently large number of turns). But the dominance of multivalent ions leads to new features of the transition such as the possibility of collapse from a completely straight DNA configuration into condensed structures such as toroids, due to the attractive-repulsive nature of the DNA-DNA interactions (see DNA Condensation: Coil-Globule Transition). Next, we outline the method to calculate the transition between the straight and supercoiled configurations that is described in detail in Argudo and Purohit (11).

Transition from straight to straight-supercoil coexistence

The transition from the straight to the straight-supercoil coexistence is characterized by a critical force $F_{critical}$ as a function of the number of turns or equivalently a critical number of turns $n_{critical}$ as a function of the applied force F. As noted in the literature (11,25,26), at the transition point there is a jump in the torque $\delta M = M_{critical} - M_3$ together with a jump in the vertical extension δz. The jump in the extension corresponds to the appearance of the end-loop and a sudden formation of a supercoil with $l_p^{critical} > = 0$, where $l_p^{critical}$ is the length of the helical region right after the transition. To find ($n_{critical}$, $F_{critical}$, δM, δz, and $l_p^{critical}$), we follow the method described in Argudo and Purohit (11). We compute the transition variables by recognizing 1), that at the transition the free energy of both configurations is equal, and 2), that the linking number $n = Lk$ is a topological invariant that must be continuous at the transition. Comparing the energies in Eqs. 9 and Eq. 1, together with $n_{c-s} = n_{c-p}$, readily yields $l_p^{critical}$, $M = M_{critical}$, $n_{critical}$, and the other transition variables.

Using proper parameters in the interaction energy $U(r, \theta)$ as calculated in Todd et al. (36), we found that as F decreases, the length of the supercoil that appears just after the transition $l_p^{critical}$ increases, and the torque just before the transition $M = M_{critical}$ decreases. Furthermore, for the force F_T, the solution to the minimization of the energy V_{p-5} yields M_3, θ, $r > 0$, and $l_p^{critical}$, $L - l_o$. Because M_3, r, and θ have nonzero values, by the use of Eqs. 5–8, it is clear that the number of turns at which the DNA molecule transitions into supercoiling is larger than zero. The number of turns $n_{critical}$ (F_T) is, in fact, equal to the minimum number

Please cite this article in press as: Argudo and Purohit, Competition between Supercoils and Toroids in Single Molecule DNA Condensation, Biophysical Journal (2012), doi:10.1016/j.bpj.2012.05.033

of turns n_{min} for which supercoiled structures can coexist with straight DNA. We point out that the numerical calculation of F_T based on comparing the energy of two states neglects the presence of thermal kicks that can lower or raise the energy barrier for the transition between states. In general, for a given force $F \geq F_T$, the transition would take place over a range of values of n. Consequently, the computed values of F_T and $n_{critical}$ at the transition are estimates. Furthermore, we know that the transition is a dynamic process that needs further study, including adequate kinetic analysis.

Transition to the fully supercoiled state: pure plectoneme

So far, in our description of the problem, we have neglected the geometric constraint $l_p \leq L - l_o$. As more turns are added, beyond $n_{critical}$, the straight l_t portion decreases and l_p increases. As a consequence of the above constraint, holding F constant, as n increases it reaches $n_{critical}$ for which supercoils and tails coexist. As n is further increased, it reaches a value $n = n_{pp} > n_{critical}$, where $l_p = L - l_o$ and the DNA has been entirely converted into a pure plectoneme. The number of turns as a function of F at which the transition into the pure plectoneme takes place is given by

$$n_{pp}(F) = n_{critical}(F) + \frac{L - l_p^{critical}(F) - l_o(F)}{dl_p(F)/dn}, \qquad (17)$$

where dl_p/d_n is the change in the length of the helices as a function of the number of imposed turns (11):

$$\frac{dl_p}{dn} = \left[\frac{\sin 2\theta}{4\pi r} - \frac{M_3}{8\pi K_b K}\right]^{-1}. \qquad (18)$$

So far, we have theoretical estimates of $n_{critical}(F)$ and $n_{pp}(F)$ in n versus F space describing DNA transitions in single molecule experiments. This would prove to be useful, as shown in the subsection Phase Diagram: DNA Configurations, to understand the description of the complete phase diagram of DNA configurations when we include the possibility of formation of not only supercoils, but also toroidal structures. So, next we consider the possibility of DNA condensation into toroidal structures under imposed tension and end-rotations.

DNA GLOBULAR STATE

Experimental studies of DNA condensation (induced by multivalent ions) in the bulk have shown that DNA condenses into toroidal structures (12–15). Consequently, the globular state is modeled as a torus. We will denote by a the radius of the tube and R the distance from the center of the tube to the center of the torus (see Fig. 1). The free energy in the globular state in the absence of twist can be found in Grosberg and Zhestkov (22,23). Here we include the possibility of applying moments to the DNA chain. The free energy of the globule is approximately given by

$$V_g = L_g\left(G_g + \epsilon\frac{K_b}{R^2} + \frac{M_g^2}{2K_t}\right) + \frac{E_s Ra}{d^2}, \qquad (19)$$

where L_g is the DNA length in the condensed-globular state. The first term in parentheses $G_g < 0$ is the energy of intersegment interaction per unit length, and is negative, due to the attractive nature of the interactions from the multivalent ions in condensed DNA (16,23,36). As stated in Todd et al. (36), there are "nominal configurational" differences between globular DNA condensates and parallel DNA strands under osmotic stress, but in both cases the intermolecular interactions between DNA filaments are the predominant effect. Minimization of the surface and bending energy in the toroidal condensates would theoretically lead to the same local structure as parallel arrays (36). Therefore $G_g = U(D_{eq})$ is the interaction energy given by Eq. 15 at the equilibrium distance (36). In the Supporting Material, we describe a different model suggested by Battle et al. (39) to account for the torus internal energy interactions that leads to similar results.

The second term in Eq. 19 is the bending energy and the entropic cost of confinement. An estimate of the confinement free energy per unit length of the toroid can be computed from the configurational cost of a long persistent chain confined into a sphere. It is approximately the bending energy of the toroid, $\sim 2K_B R^{-2}$ (40). If the configurational entropy is neglected, then $\epsilon = 1/2$ from the bending contribution. The third term in Eq. 19 is the twisting energy per unit-length, where M_g is the induced moment in globular state due to end-rotations. The parameter E_s in Eq. 19 represents the surface tension energy of a toroid of volume $\propto Ra^2$. The effective diameter of the DNA chain in the toroidal state is $d = D_{eq}$ and its value is regulated by the internal interactions of the loops making up the toroid. The free energy V_g has to be minimized subject to two constraints. The first constraint is given by the requirement that the volume of the globule (torus) in the condensed state has to be approximately equal to the volume of DNA chain (22)

$$L_g d^2 \approx cRa^2, \qquad (20)$$

where we have introduced the constant $c \in [1, 8\pi]$ to account for the prefactors in the volume of a distorted torus. Further discussion about the constant c can be found in the Supporting Material. The chain forms $\sim N_g \approx L_g/(2\pi R) = (ca^2)/(2\pi d^2)$ loops (41), also known as the "torus winding number" (39). The second constraint says that the number of turns n imposed on the DNA chain has to be equal to the linking number Lk_g (a topological invariant) of the globule

$$Lk_g = \frac{M_g}{2\pi K_t}L_g + Wr, \qquad (21)$$

Please cite this article in press as: Argudo and Purohit, Competition between Supercoils and Toroids in Single Molecule DNA Condensation, Biophysical Journal (2012), doi:10.1016/j.bpj.2012.05.033

where the first term is the twist of the chain Tw and Wr is writhe. The total writhe present in the globule is $Wr = Wr^+ - Wr^-$, where the Wr^+ expressions are the positive turns Wr^- are the negative turns under a given sign convention. However, note that the number of loops in the globule is equal to $N_g = Wr^+ + Wr^-$, such that $Wr = N_g - 2Wr^-$ and Wr^- is an unknown. Next, we introduce the constraints from Eqs. 20 and 21 via the Lagrange multipliers μ and λ:

$$\begin{aligned}\widehat{V}_g &= V_g + \mu\left(L_g - cR\frac{a^2}{d^2}\right)\\ &\quad + \lambda\left(Lk_g - \frac{M_g L_g}{2\pi K_t} - \frac{ca^2}{2\pi d^2} + 2Wr^-\right).\end{aligned} \tag{22}$$

Then energy $\widehat{V}_g$ has to be minimized with respect to the unknown variables M_g, a, R, and Wr^-. Performing $\partial\widehat{V}_g/\partial M_g$ yields $\lambda = 2\pi M_g$. The second partial derivative $\partial\widehat{V}_g/\partial a = 0$ gives

$$\mu c\frac{aA}{k_B T d} = \frac{\gamma}{2} - M_g\frac{caA}{k_B TRd}, \tag{23}$$

where $\gamma = AE_s/(k_B Td)$. The third partial derivative $\partial\widehat{V}_g/\partial R = 0$ yields

$$\frac{2\epsilon L_g}{R^3} = \frac{a}{A^2 d}\left[\gamma - \mu c\frac{aA}{k_B Td}\right], \tag{24}$$

and combining Eqs. 23 and 24, we obtain a relationship between R and a as a function of M_g:

$$\frac{2\epsilon L_g}{R^3} = \frac{a}{A^2 d}\left[\frac{\gamma}{2} + M_g\frac{cAa}{k_B TRd}\right]. \tag{25}$$

Performing $\partial\widehat{V}_g/\partial Wr^- = 0$ results in the condition $M_g = 0$, such that $Lk_g = Wr = N_g - 2Wr^-$ and there is no twist present in the globule. Setting $M_g = 0$ in Eq. 25 and using the constraint Eq. 20 we recover the solution for the size of the DNA condensate in the absence of twist (22,23),

$$\begin{aligned}R^o &\approx \frac{A}{c\alpha^{2/5}}\left(\frac{L_g}{A}\right)^{1/5},\\ a^o &\approx d\alpha^{1/5}\left(\frac{L_g}{A}\right)^{2/5},\end{aligned} \tag{26}$$

where $\alpha = \gamma/(4\epsilon c^3)$ is a constant. The globule's winding number is given by

$$N_g^o \approx \frac{ca^2}{2\pi d^2} = \alpha^{2/5}\frac{c}{2\pi}\left(\frac{L_g}{A}\right)^{4/5}, \tag{27}$$

and $Wr^- = (N_g^o - n)/2$. From the energy-minimization procedure, the obtained values of R^o and a^o yield a surface tension energy that is four times the bending energy of the system. In the case where $M_g = 0$, because the relations given in Eq. 26 are independent of the number of turns n and force F, the equilibrium energy of the globular system given by Eq. 19 is a constant independent of the controlled variables F and n.

The results in Eqs. 26 and 27 given by the condition $M_g = 0$ are independent of the number of turns n and reflect that the DNA chain can accommodate all the external applied link into the loops forming the torus. It should be noted that $Wr^- > 0$ is an independent variable as long as the number of applied turns n is smaller than the number of loops N_g^o that the globule can accommodate. When n is larger than N_g^o given by Eq. 27, the extra link that the torus cannot accommodate as loops has to be stored as twist. If $n > N_g^o$, then $Wr^- = 0$, $M_g \neq 0$ and the solution to the minimization of $\widehat{V}_g$ is given by Eq. 25 together with the constraints Eq. 20 and Eq. 21.

Note that the system will adopt the same solution with $M_g \neq 0$ in Eq. 25 for all values of n, if, due to kinetic or other constraints, the globule is forced to store single signed loops (e.g., $Wr^- = 0$). As expected for $M_g \neq 0$, the energy of the toroidal system is no longer independent of the number of turns n. Therefore we see that if $n \leq N_g^o$, then the theoretical scenario with $M_g = 0$ is the limiting case where the system is always able to reach thermodynamic equilibrium. However, if $n \geq N_g^o$, then the solution with $M_g \neq 0$ in Eq. 25 is similar to taking into account some constraints that might force single signed loops in the toroid. Finally, we point out that the results obtained following the methods described in this section are valid as long as the results yield $R > a$, for which the DNA has a toroidal structure (22).

DNA condensation: coil-globule transition

Mamasakhlisov et al. (23) recently developed a statistical mechanical model, based on a mean field approach and the Zimm-Bragg model, for the condensation of an insoluble flexible polymer under tension and no twist. According to their theory, for an infinite length chain the transition is first order, whereas for finite length polymer the transition is sharp and progresses over a small interval of tension.

To consider the straight-to-globule transition under tension and imposed end-rotations we simplify the treatment given by Mamasakhlisov et al. (23) and use a similar idea to the transition model used in Baumann et al. (16). We assume the transition to be sharp (small cooperativity value) such as in the case of the homogeneous persistent chain (23). This assumption is based on recent DNA single molecule experiments in multivalent salts done by van den Broek et al. (18), where a single nucleation cite for the toroid was observed, which leads to the idea that the surface energy term in the free energy of a toroidal condensate is indeed large. We can now compare the energy of the straight configuration (right before the transition) with the energy of the condensed-toroid (right after the transition). The energy of the condensed-torus is described in DNA Globular State

Please cite this article in press as: Argudo and Purohit, Competition between Supercoils and Toroids in Single Molecule DNA Condensation, Biophysical Journal (2012), doi:10.1016/j.bpj.2012.05.033

and is given by Eq. 19 where $L_g = L$, such that the entire DNA has collapsed and is in the toroidal state. We can estimate the value of the force F_{c-o} (as a function of the number of turns n) for which the transition (straight $\rightarrow$ toroid) occurs as done previously by noting that: 1), at the transition the energy of the straight configuration and condensed-globular configuration are equal, and 2), the linking number $Lk_g = n_{c-s} = n_{sg}$ is a topological invariant that must be continuous at the transition. First we consider the case where $n \leq Wr_g^o$ together with $M_g = 0$. Comparison of the energies given by Eqs. 1 and 19 together with the requirement of no twist in the globular region yields the relationship between the transition force F_{c-o} and the number of turns n_{sg} at the transition,

$$F_{c-o} = \frac{M^2}{2K_t} + G^*_{flu} + \frac{M^2}{4K_bK} - G_g - 5\epsilon K_b \left(\frac{c^5\alpha^2}{A^4 L_g}\right)^{2/5}, \quad (28)$$

where a^o and R^o have been replaced with the solution given in Eq. 26. The value of the moment M in the straight configuration is prescribed as a function of the number of turns at the transition n_{sg} given by Eq. 4.

In the case where $n \geq Wr_g^o$ or in the case when the torus can only store one signed turns, comparison of the energies between the two states yields the critical force as a function of the number of turns n_{sg}^{twist},

$$F_{c-o}^{twist} = \frac{M^2 - M_g^2}{2K_t} + G^*_{flu} + \frac{M^2}{4K_bK} - G_g - \epsilon\frac{K_b}{R^2} - \frac{E_s R a}{L d^2}, \quad (29)$$

where M_g, a, and R are given by solving the system of equations presented in Eqs. 20, 21, and 25 and M is given by Eq. 4 as a function of the number of turns at the transition in the presence of twist n_{sg}^{twist}.

We close this section by pointing out that although the step size in single-molecule experiments may be dictated by a kinetic process, we are interested in the final loop sizes governed by the thermodynamic parameters. We assume that, for sufficiently long waiting times, DNA will reach thermodynamic equilibrium. Our assumption is supported by the experimental studies (12–14) in the bulk under the introduction of static loops and the computer simulations in Cárdenas-Lizana and Hsiao (42). For a brief discussion of the final size of the toroid, we refer the reader to the Supporting Material.

RESULTS

Comparison with experiment

The experiments by Besteman et al. (5,43) were performed for a DNA sample of length $L \approx 2720$ nm and for three different condensing agents: spermine, cosep, and protamine. To see if we can fit their data we started by solving the transition from straight DNA to supercoiled-straight configuration. For the twisting modulus, we have used $K_t \sim 86\ k_BT$ as done by Besteman et al. (5), whereas for the bending modulus we have used $K_b \sim 50\ k_BT$ for spermine (as done in Besteman et al. (5) and van den Broek et al. (18)), and $K_b \sim 25\ k_BT$ both for cosep and protamine. There is evidence that there is a substantial decrease in the bending modulus in the presence of condensing agents, where cations with higher charge density have a stronger effect (44). The bending moduli have been measured to decrease up to $K_b \sim 15\ k_BT$ for strong condensing agents such as cohex (16). For the intersegment equilibrium distance $d = D_{eq}$, we have used $D_{eq} = 2.815$ nm for spermine as measured by Todd et al. (36), $D_{eq} = 2.7$ nm for protamine as done in Besteman (43) and approximated $D_{eq} = 2.7$ nm for cosep based on the measured value for other condensing agents (36).

The phenomenological parameters C_A and C_R used for the condensing agents were obtained as estimates from the measurements performed for different condensing ions in Todd et al. (36). Finally, for the decay length λ we have used for spermine and cosep $\lambda = 0.46$ nm as done in Todd et al. (36) and for protamine we have used $\lambda \approx 0.485$ nm, which is consistent with the values used by DeRouchey and Rau (10). The blue solid line in Figs. 2 and 3 shows the transition from straight $\rightarrow$ straight-supercoiled as a function of the controlled variables F and n. Our theoretical predictions accurately match experiment for moderately large numbers of turns. The black dashed line shows the minimum number of turns n_{min} for which supercoiled structures coexist with straight DNA portions (plectonemes with tails). For $n < n_{min}$ there is no solution to the transition problem straight $\rightarrow$ straight-supercoiled. Interestingly, the theoretical value of n_{min} appears to agree with a discontinuous jump in the data of Besteman et al. for the condensing

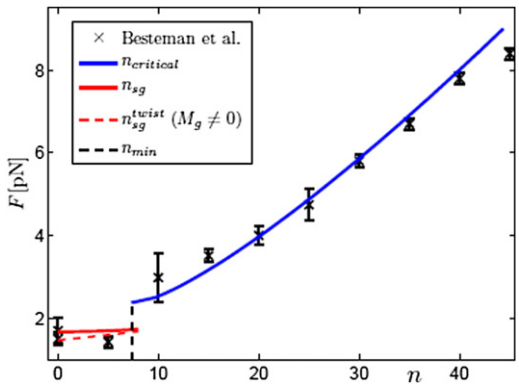

Web 3C

FIGURE 2 Curve of $n_{critical}$ shows the transition from straight configuration to supercoiled + straight coexistence. The curve n_{min} shows the minimum number of turns at which supercoiled + straight can coexist. The curve n_{sg}^{twist} (n_{sg} for toroids with no twist) shows the transition from straight to toroidal configurations. Spermine is the condensing agent, and we have used $C_A = 690$ pN/nm^2, $K_b = 50\ k_BT$, and $\alpha = 0.013$ ($\beta = 2.6$ and $\Gamma d^2/(k_BT) \approx 0.6$).

Please cite this article in press as: Argudo and Purohit, Competition between Supercoils and Toroids in Single Molecule DNA Condensation, Biophysical Journal (2012), doi:10.1016/j.bpj.2012.05.033

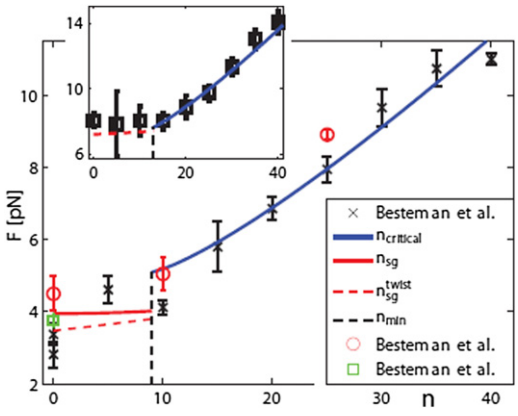

FIGURE 3 Same predictions as in Fig. 2, but using cosep as the condensing agent. We have used $C_A = 1150$ pN/nm^2, $K_b = 25\ k_BT$, and $\alpha = 0.013$ ($\beta \approx 7.5$ and $\Gamma d^2/(k_BT) \approx 1.1$). (*Black crosses*, *green squares*, and *red circles*) Experimental data in Besteman et al. (5) for different molecules under same experimental conditions. (*Inset*) Comparison to the experimental data using protamine as the condensing agent (43). For protamine we have used $\beta = 1$ and the same values of C_A, D_{eq}, and K_b as the ones used for cosep, because both condensing agents have a high charge density. Using K_b as low as 15 k_BT still gives very good agreement with experiment for both protamine and cosep.

agents, where there seems to be a region of experimental points that is approximately independent of n (zero slope) and region where the points increase as a function of n.

Next, we consider the possibility that DNA molecules can collapse into toroidal structures for both spermine and cosep. We use the same electrostatic parameters (C_A, C_R, D_{eq}) and bending modulus K_b that we used for the straight-to-supercoil transition. We neglect here the confinement cost in toroidal structures and set $\epsilon = 1/2$ (the effect of ϵ and other parameters on the calculations is described in the Supporting Material).

The only parameter left is the surface tension term $\alpha(E_s \propto \alpha)$ in the free energy of the torus. The surface energy contribution for DNA condensates has not been completely worked out in the literature and we could not find specific values for any condensing agent. In one of their articles, Ubbink and Odjik (45) suggest that the surface tension energy $E_{surface} \approx Ak_BT\ V^{1/3}\ d^{-2}$ becomes important when the dimensionless parameter $\beta \sim O(1)$, where $V = \pi L(d/2)^2$ is the volume of the torus. Using our notation,

$$\beta = 4\epsilon(cd)^2\ V^{-1.3}\ \left(\alpha^4 L^3 A^{-8}\right)^{1/5}.$$

In another article, Ubbink and Odjik (46) suggest that for $E_{surface} \approx \Gamma S$, where Γ is the surface tension parameter and $S = (2\pi)^2\ Ra$ is the surface area of the torus, $\Gamma d^2/(k_BT) \sim O(1)$. In our notation,

$$\frac{\Gamma S}{(k_BT)} \approx 4\epsilon c^2\ \left(\alpha^4 L^3 A^{-3}\right)^{1/5}.$$

In their work on condensation, Park et al. (41) used estimates of the cohesive energy where $E_{surface} = \Gamma S$ and $\Gamma d^2/(k_BT) \approx 0.06 \sim O(1/100)$. The values used by Park et al. and those suggested by Ubbink and Odjik differ greatly in magnitude. Finally, in Cherstvy (40), the surface tension parameter is suggested to be $|E_o| \in [0.1\text{–}0.5]$ nm^{-1}, where our parameter is $\alpha \propto |E_o|\ Ac^{-5/2}$. Due to the wide range of suggested values for the surface tension parameter we take α as a fit to the point $n = 0$ in the experiments of Besteman et al. (5). To validate the fitted value of α we compare it to the previously suggested values of the surface tension in the literature (40,41,45,46), using them as upper and lower bounds. For both condensing agents in Figs. 2 and 3 the fitted value is $\alpha = 0.013$. This means $\beta \approx 2.6$ and $\Gamma d^2/(k_BT) \approx 0.6$ for spermine, whereas $\beta \approx 7.5$ and $\Gamma d^2/(k_BT) \approx 1.1$ for cosep, because $d = D_{eq}$ and A depend on the condensing agent. In both cases, the surface tension parameter is of the order suggested by Ubbink and Odjik (45,46).

The red solid line in Figs. 2 and 3 shows the transition from straight → toroids (with no twist) as a function of the controlled variables F and n. The red dashed line shows the transition for toroids with twist. Our theoretical predictions show good quantitative agreement with experiment for $0 < n < n_{min}$. The solution to the problem in thermodynamic equilibrium shows that the supercoiled-straight configurations are energetically more favorable than the toroidal condensates for $n \geq n_{min}$ and $F > 0$.

The solution to the problem in thermodynamic equilibrium where supercoiled structures compete with toroidal condensates is given by a comparison of the energies Eq. 9 and Eq. 19. In the Supporting Material, we address how this competition of DNA configurations plays out as a function of persistence length A, the toroid configurational entropy parameter ϵ, and the toroid surface tension parameter α.

In the next section, we complete a phase diagram based on the DNA configurations we studied.

Phase diagram: DNA configurations

Fig. 4 *a* shows a schematic of a phase diagram as a function of the controlled variables (F, n). We have used the theoretical solution for the description of the experiments in Besteman et al. (5) in spermine (see Comparison with Experiment). For the labeling of each region, see the caption of Fig. 4. The light-blue region labeled U is an unknown region in the phase diagram. The minimization of energy over the studied configurations does not yield a favorable state in the unknown region. In this region, $F \leq F_T$ such that there are no supercoiled-straight configurations and the number of turns n is not sufficiently large to consider a pure plectonemic state where the energy is approximately independent of F. The unknown region is below the yellow region (which corresponds to a collapsed DNA structure), yet based on our theoretical analysis of constrained minimization, in parts of the unknown region the straight

Please cite this article in press as: Argudo and Purohit, Competition between Supercoils and Toroids in Single Molecule DNA Condensation, Biophysical Journal (2012), doi:10.1016/j.bpj.2012.05.033

Web 3C

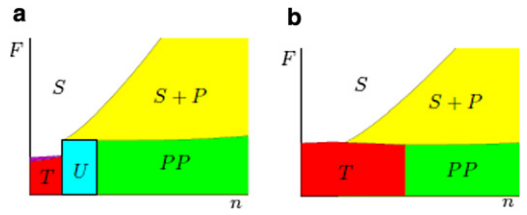

FIGURE 4 Phase diagrams constructed using the theoretical solution for the description of Besteman et al. (5) experiments in spermine. (*a*) We used $\alpha = 0.013$ as in Fig. 2 and (*b*) $\alpha = 0.0003$. The straight configuration is the most favorable one in the white region and it is marked with *S*. The straight-supercoiled configuration is marked with $S + P$ (*yellow*), whereas the entirely supercoiled structure (pure plectonemes) is marked with *PP* (*green*). *T* stands for the region where we expect to see toroidal structures. (*Red*) Region where we expect to see toroids, with or without twist, and (*purple*) region where we expect to only see toroids without twist. (*Light-blue region* labeled *U* in panel *a*) Unknown region where there is no clear favorable configuration.

configurations are preferred to toroidal structures. This would mean that as F is decreased, the DNA can collapse into supercoiled structures and as F is further reduced, then it will go back to a straight configuration. This seems counterintuitive, so we identified this region as unknown. We suspect that in the unknown region, toroids and plectonemes compete and that the configurations in this region are more complex forms of DNA compaction, which can be clarified by further experiments or simulations.

The solution for straight $\rightarrow$ straight-supercoiled configurations for $F \sim F_T$ yields helices with large pitch $2\pi r \cot\theta$ ($\theta \rightarrow 0$), meaning that the DNA is approaching the configuration of two parallel rods. The value of the supercoiling angle θ is nearly constant for $F > F_T$, but as $F \rightarrow F_T$ the value of the supercoiling angle θ decreases sharply as depicted in Fig. S1. As the pitch increases the two DNA filaments see each other less and it is expected that the magnitude of the internal interactions will decrease. This is the case for DNA in monovalent salt solutions as evidenced by the energy expressions provided by Ubbink and Odjik (37). Therefore even though for $F > F_T$ the phenomenological model $U_{es}(r)$ given in Eq. 15 for the helical region provides good estimates when compared to experiment, this approximation should become less accurate for F close to F_T. For $F \sim F_T$, the internal energy becomes less negative, and we expect the actual value of the transition force F to decrease when compared to the theoretical case used to construct the phase diagram in Fig. 4 *a*.

Considering this effect would modify the $S \rightarrow S + P$ transition curve close to the region $F \sim F_T$ and $n \sim n_{min}$ in Fig. 4 *a*. Consequently, we expect our theoretical solution for the transition close to F_T to provide some qualitative insight to the transition problem rather than an accurate prediction. In Schnurr et al. (47) and Montesi et al. (48), the authors provided a thorough analysis of a collapse of single, stiff polymers in poor solvent in the absence of twist and tension. It was suggested that the condensation proceeds via a cascade through metastable intermediates (i.e., racquets) toward the equilibrium configuration that is the torus. We speculate that the high-pitch solutions (that approach two parallel filaments) resemble the racquets studied in Schnurr et al. (47) and Montesi et al. (48).

In Fig. 4 *b* we show a scenario where we have decreased the surface tension parameter $\alpha = 0.0003$ (~40 times smaller than the one used to fit the experiments of Besteman et al.). The solution yields toroids of mean radius $R \sim 120$ nm. We can see that there is a region in (F, n) space, where DNA makes a transition straight-supercoiled $\rightarrow$ toroid and that there is no unknown region. The unknown region tends to disappear for $\alpha < \sim 0.001$ ($\Gamma d^2 \sim 0.1\ k_B T$), which is of the order of the value used by Park et al. (41) and an order-of-magnitude lower than the ones used to fit the data of Besteman et al. (5) in Fig. 4 *a*.

CONCLUSIONS

We have studied the mechanics of DNA in the presence of condensing agents. The result of our analysis is a phase diagram showing the most favorable DNA configuration as a function of the controlled variables—force F and number of turns n. Because the possible physical mechanisms of counterion-induced DNA condensation are still debated in the literature (9,36), our theoretical-mechanical model can be used as a framework to test DNA-DNA interaction theories. Our model allows to easily see the effects of parameters such as K_b and D_{eq} (which are specific to the condensing agent and its concentration (36,44)) on the final equilibrium structure. We have constrained our analysis to the observed DNA configurations—straight, supercoiled, and toroidal. Here we give a short summary of all the results we have obtained.

A key result of our analysis is that there are no supercoiled solutions to the equations of equilibrium below a critical force F_T in the presence of condensing agents (see Fig. S1). For moderately large values of n and F (not too close to F_T) the supercoiled structures are the most favorable state, but as the number of turns increases (or tensile force decreases for moderately large n) there is a transition into pure plectoneme. For low values of n, toroidal structures are favored when $F < F_T$. Our theoretical estimates of the transition force and number of turns n describe the experiments of Besteman et al. very accurately away from the point $F \sim F_T$ and $n \sim n_{min}$. The predicted DNA configurations from our phase diagram can be tested experimentally using fluorescence imaging methods to visualize the formation of the collapsed structure as done in (18).

Also, if there is formation of supercoiled structures, this process should be reversible and therefore there would be no hysteresis in the loading and unloading curves as long as the supercoils persist. This is the case in the formation of plectonemic structures in monovalent salt (24,26,49), when there are no structural changes in the DNA molecule

Please cite this article in press as: Argudo and Purohit, Competition between Supercoils and Toroids in Single Molecule DNA Condensation, Biophysical Journal (2012), doi:10.1016/j.bpj.2012.05.033

(20,50,51). Furthermore, as noted in Fig. S1, our model predicts that for moderately large F the slopes of the hat curves (extension versus rotation) are relatively constant as a function of n, whereas the value of the slope sharply increases as F decreases approaching F_T. The same methods used to measure the torque and slope in single-molecule experiments using monovalent salts can be used in the presence of condensing agents and therefore test our theoretical predictions.

Our treatment of the toroidal structures assumes a large continuum limit where $R > a >> D_{eq}$ with no geometrical defects. The final toroidal state depends on the value of the surface tension parameter α whose value remains unresolved. In Fig. 2, the red solid line showing the transition from straight → toroids, matches quantitatively the experimental data. But the match between theory and experiment is not so obvious in Fig. 3, where experiment shows a large range of force values for $n = 0$ and $n = n_{min}$ at the transition from straight → toroids. Changing the value of α (while still inside the range used previously in the literature (41,45,46)), modifies the phase diagram (see Fig. 4) for low values of F and n. Using different values of α can reproduce the entire range of values of the experiments in Besteman et al. in Fig. 3.

Possible improvements to our theoretical framework include modeling thicker toroids when $R \sim a$ (52), deformed toroids (45), and toroidal structures with topological defects (41). Also note we have performed only a constrained minimization of the free energy over a class of equilibrium structures, which leads to a region in the phase diagram where the preferred configuration is unknown. More sophisticated calculations and experiments will be needed to determine the correct equilibrium shape of the DNA in that region.

SUPPORTING MATERIAL

Additional sections with six figures are available at http://www.biophysj.org/biophysj/supplemental/S0006-3495(12)00613-3.

We acknowledge partial support through a National Science Foundation CAREER award (grant No. NSF CMMI-0953548) and through the Nano/Bio Interface Center at the University of Pennsylvania through grant No. NSF DMR08-32802.

REFERENCES

1. Bloomfield, V. A. 1997. DNA condensation by multivalent cations. *Biopolymers.* 44:269–282.
2. Rau, D. C., and V. A. Parsegian. 1992. Direct measurement of the intermolecular forces between counterion-condensed DNA double helices. Evidence for long range attractive hydration forces. *Biophys. J.* 61:246–259.
3. Raspaud, E., D. Durand, and F. Livolant. 2005. Interhelical spacing in liquid crystalline spermine and spermidine-DNA precipitates. *Biophys. J.* 88:392–403.
4. Burak, Y., G. Ariel, and D. Andelman. 2004. Competition between condensation of monovalent and multivalent ions in DNA aggregation. *Curr. Opin. Colloid Interface Sci.* 9:53–58.
5. Besteman, K., S. Hage, …, S. G. Lemay. 2007. Role of tension and twist in single-molecule DNA condensation. *Phys. Rev. Lett.* 98: 058103.
6. Murayama, Y., Y. Sakamaki, and M. Sano. 2003. Elastic response of single DNA molecules exhibits a reentrant collapsing transition. *Phys. Rev. Lett.* 90:018102.
7. Thomas, T., and T. J. Thomas. 2001. Polyamines in cell growth and cell death: molecular mechanisms and therapeutic applications. *Cell. Mol. Life Sci.* 58:244–258.
8. Brewer, L. 2011. Deciphering the structure of DNA toroids. *Integr. Biol.* 3:540–547.
9. Kornyshev, A. A., D. J. Lee, …, A. Wynveen. 2007. Structure and interactions of biological helices. *Rev. Mod. Phys.* 79:943–996.
10. DeRouchey, J. E., and D. C. Rau. 2011. Role of amino acid insertions on intermolecular forces between arginine peptide condensed DNA helices: implications for protamine-DNA packaging in sperm. *J. Biol. Chem.* 286:41985–41992.
11. Argudo, D., and P. K. Purohit. 2012. The dependence of DNA supercoiling on solution electrostatics. *Acta Biomater.* 8:2133–2143. 10.1016/j.actbio.2012.01.030.
12. Shen, M., K. Downing, …, N. Hud. 2000. Nucleation of DNA condensation by static loops: formation of DNA toroids with reduced dimensions. *J. Am. Chem. Soc.* 122:4833–4834.
13. Hud, N. V., K. H. Downing, and R. Balhorn. 1995. A constant radius of curvature model for the organization of DNA in toroidal condensates. *Proc. Natl. Acad. Sci. USA.* 92:3581–3585.
14. Conwell, C. C., I. D. Vilfan, and N. V. Hud. 2003. Controlling the size of nanoscale toroidal DNA condensates with static curvature and ionic strength. *Proc. Natl. Acad. Sci. USA.* 100:9296–9301.
15. Hud, N. V., and I. D. Vilfan. 2005. Toroidal DNA condensates: unraveling the fine structure and the role of nucleation in determining size. *Annu. Rev. Biophys. Biomol. Struct.* 34:295–318.
16. Baumann, C. G., V. A. Bloomfield, …, S. M. Block. 2000. Stretching of single collapsed DNA molecules. *Biophys. J.* 78:1965–1978.
17. Fu, W. B., X. L. Wang, …, M. Li. 2006. Compaction dynamics of single DNA molecules under tension. *J. Am. Chem. Soc.* 128:15040–15041.
18. van den Broek, B., M. C. Noom, …, G. J. Wuite. 2010. Visualizing the formation and collapse of DNA toroids. *Biophys. J.* 98:1902–1910.
19. Fu, W., H. Chen, …, J. Yan. 2010. Kinetics of single DNA compaction by hexamine cobalt chloride. *J. Comput. Theor. Nanosci.* 7:213–217.
20. Bryant, Z., M. D. Stone, …, C. Bustamante. 2003. Structural transitions and elasticity from torque measurements on DNA. *Nature.* 424: 338–341.
21. Moroz, J., and P. Nelson. 1998. Entropic elasticity of twist-storing polymers. *Macromolecules.* 31:6333–6347.
22. Grosberg, A. Y., and A. V. Zhestkov. 1986. On the compact form of linear duplex DNA: globular states of the uniform elastic (persistent) macromolecule. *J. Biomol. Struct. Dyn.* 3:859–872.
23. Mamasakhlisov, Y. Sh., B. A. Todd, …, V. A. Parsegian. 2009. DNA stretching and multivalent-cation-induced condensation. *Phys. Rev. E.* 80:031915.
24. Forth, S., C. Deufel, …, M. D. Wang. 2008. Abrupt buckling transition observed during the plectoneme formation of individual DNA molecules. *Phys. Rev. Lett.* 100:148301.
25. Daniels, B. C., S. Forth, …, J. P. Sethna. 2009. Discontinuities at the DNA supercoiling transition. *Phys. Rev. E.* 80:040901.
26. Brutzer, H., N. Luzzietti, …, R. Seidel. 2010. Energetics at the DNA supercoiling transition. *Biophys. J.* 98:1267–1276.
27. Fuller, F. B. 1971. The writhing number of a space curve. *Proc. Natl. Acad. Sci. USA.* 68:815–819.

Please cite this article in press as: Argudo and Purohit, Competition between Supercoils and Toroids in Single Molecule DNA Condensation, Biophysical Journal (2012), doi:10.1016/j.bpj.2012.05.033

28. Thompson, J., G. van der Heijden, and S. Neukirch. 2002. Supercoiling of DNA plasmids: mechanics of the generalized ply. *Proc. R. Soc. Lond. A.* 458:959–985.

29. Clauvelin, N., B. Audoly, and S. Neukirch. 2009. Elasticity and electrostatics of plectonemic DNA. *Biophys. J.* 96:3716–3723.

30. Purohit, P. K. 2008. Plectoneme formation in twisted fluctuating rods. *J. Mech. Phys. Solids.* 56:1715–1729.

31. Maffeo, C., R. Schöpflin, …, R. Seidel. 2010. DNA-DNA interactions in tight supercoils are described by a small effective charge density. *Phys. Rev. Lett.* 105:158101.

32. Neukirch, S., and J. F. Marko. 2011. Analytical description of extension, torque, and supercoiling radius of a stretched twisted DNA. *Phys. Rev. Lett.* 106:138104.

33. Kulić, I. M., H. Mohrbach, …, H. Schiessel. 2007. Equation of state of looped DNA. *Phys. Rev. E.* 75:011913.

34. Purohit, P. K., M. M. Inamdar, …, R. Phillips. 2005. Forces during bacteriophage DNA packaging and ejection. *Biophys. J.* 88:851–866.

35. Purohit, P. K., J. Kondev, and R. Phillips. 2003. Mechanics of DNA packaging in viruses. *Proc. Natl. Acad. Sci. USA.* 100:3173–3178.

36. Todd, B. A., V. A. Parsegian, …, D. C. Rau. 2008. Attractive forces between cation condensed DNA double helices. *Biophys. J.* 94: 4775–4782.

37. Ubbink, J., and T. Odijk. 1999. Electrostatic-undulatory theory of plectonemically supercoiled DNA. *Biophys. J.* 76:2502–2519.

38. van der Maarel, J. R. C. 2008. Introduction to Biopolymer Physics. World Scientific, Singapore.

39. Battle, C., B. van den Broek, …, F. C. MacKintosh. 2009. Unraveling DNA tori under tension. *Phys. Rev. E.* 80:031917.

40. Cherstvy, A. 2005. Structure of DNA toroids and electrostatic attraction of DNA duplexes. *J. Phys. Condens. Matter.* 17:1363–1374.

41. Park, S. Y., D. Harries, and W. M. Gelbart. 1998. Topological defects and the optimum size of DNA condensates. *Biophys. J.* 75:714–720.

42. Cárdenas-Lizana, P., and P. Hsiao. 2009. Stick-release pattern in stretching single condensed polyelectrolyte toroids. *Macromolecules.* 42:3211–3214.

43. Besteman, K. 2006. Charge inversion and DNA condensation by multivalent ions. PhD thesis. Technische Universiteit Delft, Delft, The Netherlands.

44. Rouzina, I., and V. A. Bloomfield. 1998. DNA bending by small, mobile multivalent cations. *Biophys. J.* 74:3152–3164.

45. Ubbink, J., and T. Odijk. 1996. Deformation of toroidal DNA condensates under surface stress. *Europhys. Lett.* 33:353–358.

46. Ubbink, J., and T. Odijk. 1995. Polymer- and salt-induced toroids of hexagonal DNA. *Biophys. J.* 68:54–61.

47. Schnurr, B., F. Gittes, and F. C. MacKintosh. 2002. Metastable intermediates in the condensation of semiflexible polymers. *Phys. Rev. E.* 65: 061904.

48. Montesi, A., M. Pasquali, and F. C. MacKintosh. 2004. Collapse of a semiflexible polymer in poor solvent. *Phys. Rev. E.* 69:021916.

49. Mosconi, F., J. F. Allemand, …, V. Croquette. 2009. Measurement of the torque on a single stretched and twisted DNA using magnetic tweezers. *Phys. Rev. Lett.* 102:078301.

50. Strick, T. R., J. F. Allemand, …, V. Croquette. 1998. Behavior of supercoiled DNA. *Biophys. J.* 74:2016–2028.

51. Strick, T., J. Allemand, …, D. Bensimon. 2000. Twisting and stretching single DNA molecules. *Prog. Biophys. Mol. Biol.* 74:115–140.

52. Pereira, G. G., and D. R. M. Williams. 2001. Toroidal condensates of semiflexible polymers in poor solvents: adsorption, stretching, and compression. *Biophys. J.* 80:161–168.

Supporting Material
Competition between supercoils and toroids in single molecule DNA condensation

David Argudo
Mechanical Engineering and Applied Mechanics,
University of Pennsylvania, Philadelphia, PA

Prashant K. Purohit [1]
Mechanical Engineering and Applied Mechanics,
University of Pennsylvania, Philadelphia, PA

[1]Corresponding author. Address: Mechanical Engineering and Applied Mechanics, University of Pennsylvania, Philadelphia, PA 19104, U.S.A., Tel.: (215)898-3870, Fax: (215)573-6334

S.1 Solution for the supercoiling parameters

Comparing the different types of lines in Fig. S1 shows how the solution for the supercoiling variables M_3, θ, r and $d\Delta z/dn$ (slope of the extension vs. rotation curves) varies as a function of the constant parameters C_A, D_{eq}, K_b. The effect of C_A can be seen by comparison of the black solid line and the blue dashed-dot line, the effect of K_b can be seen by comparison of the black solid line and the green dotted line. The slope $d\Delta z/dn$ of the hat-curves (which can be experimentally measured (1–3)), showing the end to end distance as a function of the applied number of turns is equal to $\rho dl_p/dn$, where

$$\rho = 1 - \frac{1}{2\sqrt{K_3^2 - (1/32)}} + \frac{K_b}{k_B T K_3^2 l_t} \tag{S1}$$

is the effective mean extension due to thermal fluctuations (4), K_3 is given by Eq. 2 (replacing M by M_3) in the main text and dl_p/dn is given by Eq. 18 in the main text.

S.2 Final size of the toroid at equilibrium

In constrained single molecule experiments with condensing agents, stepwise folding and unfolding signals have been obtained. The step sizes observed are believed to be correlated to the size of the toroidal structures. The measurements of Murayama et al. (5) and Fu et al. (6) show $\sim$ 300 nm step sizes yielding toroids with mean radius of $\sim$ 50 nm, similar to those observed in bulk experiments. More recently, higher resolution experiments have addressed the folding dynamics in the condensing process (7–9) yielding consistent step size of approximately $40 - 50$ nm. Based on this last set of data it has been proposed that the final step size of the toroidal condensates may be dictated by kinetic processes rather by the thermodynamic parameters (8). In Fig. S2 we plot the toroid dimensions as a function of the number of turns n. Our predicted values of R are comparable to the ones observed in experiments with unconstrained DNA (10, 11), but do not seem to agree with the step size (loop size in a toroid) measured in (7–9), which correspond to values of $R \approx 7$nm. Such small values of R would lead to a bending energy much larger (10 to 20 times larger than our predictions). The step size for $n = 0$ measured in refs. (7–9) is approximately equal to the homoclinic loop size (12).Based on these results, Besteman et al. (9) present a simple kinetic transition model with only one fitting parameter that reproduces their experimental findings very accurately. Their model is based

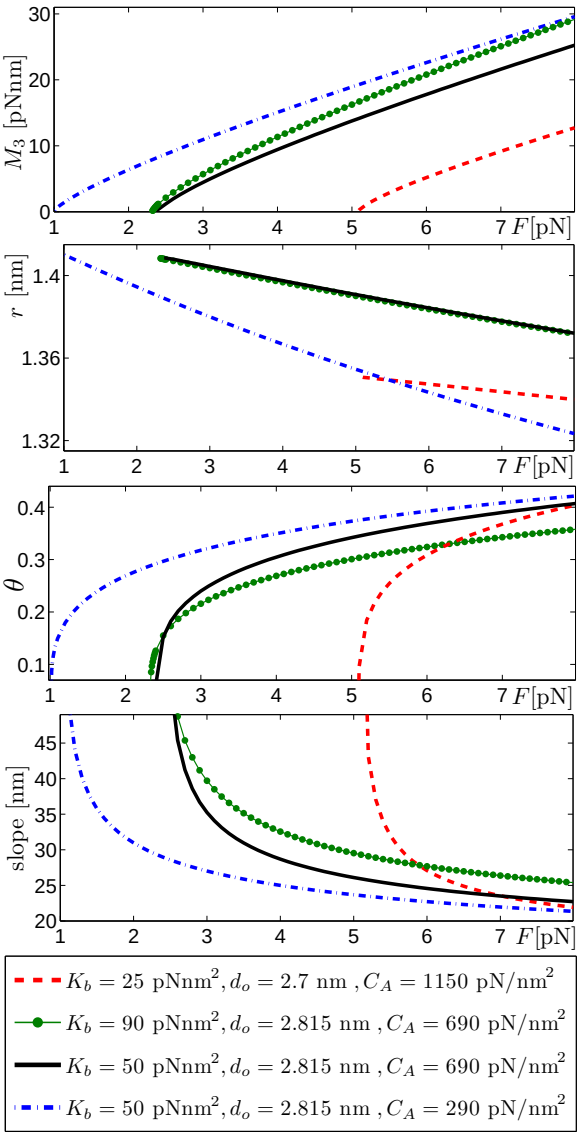

Figure S1: An increase in C_A: (a) increases the threshold force F_T, (b) decreases M_3 and θ, (c) increases $d\Delta z/dn$, and (d) causes r to deviate less from the constant value $D_{eq}/2$. An increase in K_b: (a) slightly decreases F_T, (b) causes no significant difference in r (lines are almost on top of each other), (c) decreases θ, and (d) increases both M_3 and $d\Delta z/dn$. An increase in D_{eq}: (a) significantly decreases F_T, (b) shifts the solutions for θ and M_3 to the left along the force axis, (c) increases r, and (d) decreases $d\Delta z/dn$. We have used $K_t = 86 k_B T$.

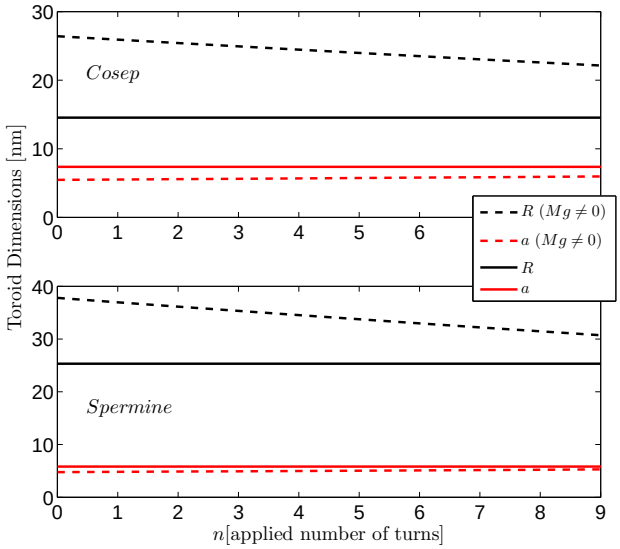

Figure S2: Toroid dimensions as a function of the applied number of turns n. The solid lines correspond to the solution for toroids with no twist and dashed lines to toroids with twist.

on the circular end loop model proposed by Strick et al. (13) and although it agrees with the experimental data it is not sufficient to predict the final configuration of the DNA molecule, since assuming a circular loop can be applicable to plectonemes, toroids or a series of separated loops (curls). In (11, 14, 15) nucleation of condensates in free DNA in the bulk was analyzed under the introduction of static loops that modified the dimensions of the toroids. It was found that static loop serves as a nucleation site that defines the average size of the final toroidal structure, which was smaller than the toroids seen in the absence of the static loops. In the same experiment it was also found that the formation of the regular size toroids (R $\approx$ 50nm) is not blocked by the introduction of the static loops. When longer waiting times were allowed, fewer smaller toroids whose size was dictated by the presence of the static loops were observed and more regular size toroids were formed. This suggests that smaller toroids are metastable states and when longer times are allowed the system approaches thermodynamic equilibrium.

Fig.S2 shows the toroid dimensions as a function of the number of turns n. The predicted values of R and a are of the same order as the ones observed in experiments with unconstrained DNA $R \sim$ 50nm and $a \sim$ 25nm (10, 11).

S.3 Alternative energy expressions for the toroidal condensates

We can also use the internal energy expression $U = H_{int}$ as suggested by Battle et al. (16) to obtain similar results for the scaling behavior of R_o and N_g^o as in the main text. In the case of the toroids we replace the electrostatic energy term $G_g L$ and the energy associated with the surface tension E_s in the energy expression Eq.22 of the main text, with Battle et al. expressions such that:

$$V_g = \omega L \left(-3 + 2\sqrt{\frac{3}{N_g}} \right) + \epsilon L \frac{K_B}{R^2}, \tag{S2}$$

where we have used the approximation of large-N_g behavior (16) and ω is the surface tension parameter. The equilibrium variables are obtained by minimizing the energy with respect to the linking number constraint Eq. 24 in the main text and the length constraint $L = 2\pi R N_g$. In the case of $M_g = 0$ we obtain:

$$R^o = \left(\frac{2\epsilon^2 K_B^2 L}{3\pi\omega^2} \right)^{1/5}, \quad N_g^o = \left(\frac{3\omega^2}{4\epsilon^2 K_B^2} \right)^{1/5} \left(\frac{L}{2\pi} \right)^{4/5}. \tag{S3}$$

The value of ω can be fitted to the case when $n = 0$ to obtain the experimental value of $F_{critical}$ in (9). Using values of $\epsilon \in [1/2, 5/2]$, for spermine $\omega \sim 0.75$pN and for cosep $\omega \sim 1.65$pN gives good fits to experiment yielding toroids of radius $R \sim 30$nm (Battle et al. uses $\omega = 1.6$pN).

S.4 Competition of Globules vs Plectonemes

For $n, F > 0$ there could be a competition between globules and plectonemes. The solution to the problem in thermodynamic equilibrium is therefore given by a comparison of the energies Eq. 9 and Eq. 22 (see main text) as a function of the state variables F and n. Figs. S3 and S4 present the energy density of competing structures as a function of the number of turns n for surface tension parameters $\alpha = 0.0013$ and $\alpha = 0.0003$ respectively. Figs. S3 and S4 show the type of energy comparison calculations done to obtain Figs. 2-4 in the main text. The values of the energetic contributions $U(r, \theta)$, G_g and the surface tension contribution E_s are not precisely known. There are other energy terms that could be important in describing each configuration such as the energy cost due to defects in the toroid (17) or a more

rigorous analysis of the energy cost upon confinement into condensed structures. Consequently, the comparison between these two states is not straight forward and could lead to more than one scenario. Below we describe the results obtained for some theoretically possible cases.

- We performed a calculation where we varied the persistence length $A \in [5\text{nm}, 150\text{nm}]$. The bending energy in the plectonemic state decreases linearly with the persistence length, while the bending energy and the surface tension energy of the torus with no twist is proportional to $A^{1/5}$. So as A increases (decreases) the increase (decrease) of the supercoiled configuration energy V_{s-p} is larger than the increase (decrease) of the torus energy $V_g(M_g = 0)$. For small values of the persistence length A the equilibrium radius R^{tw} for toroids with twist ($M_g \neq 0$) is much larger the equilibrium radius R^o of the toroids with no twist ($M_g = 0$). Toroids with twist have a larger energy than the ones with no twist. But as A increases then $R^{tw} \to R^o$ and the gap in the energy between toroids with and without twist decreases.

- We also modified the parameter $\epsilon \in [1/2, 5/2]$ to account for configurational entropy cost of the toroidal condensates, where $\epsilon = 5/2$ if the energy cost is equal to confining a flexible chain in a sphere of radius R (18). For larger values of ϵ (keeping all the other parameters fixed including α) the energy of the toroid increases, but note that the dimensions of the toroid without twist do not vary (see Eq. 29 in the main text). For larger values of ϵ we can still accurately model Besteman et al. experimental data by fitting a smaller value of α (which is still in agreement with the range given in Refs. (17–20)).

- We also computed the solution to the minimization of energy of the toroidal structure for different values of the surface tension parameter α. It is interesting to note that since $\alpha \propto c^{-5/2}$, for toroids with $M_g = 0$ and $M_g \neq 0$, the equilibrium radius R, the winding number N_g and the energy of the toroid V_g are independent of the value of the constant $c \in [1, 8\pi]$ (which stands for the shape imperfections of the toroid), but the thickness of the torus a is proportional to $c^{-1/2}$. As α decreases the toroid energy decreases and the the globular condensates become more energetically favorable. But as α decreases the globule winding number N_g^o decreases too, making toroids with out twist less likely to exist as a function of the number of turns n. Toroidal configurations start to compete with plectonemic structures for very small values of α (approximately an order of magnitude smaller than the

ones used to compare to Besteman et al. experiments). For such values of α, the solution to the minimization of energy leads to equilibrium configuration where $R \sim 100$nm for $n = 0$. For $n > n_{min}$, as F gradually decreases, even in the case where $\alpha \to 0$ (such that $N_g^o \to 0$ and $R \to 2\pi L$), straight DNA first transforms into a supercoiled-straight configuration and eventually can make a transition into a toroidal structure. So for a certain range of n the DNA makes a transition from a straight-supercoiled configuration into a toroid instead of becoming a pure plectoneme, meaning that there could be competition between pure plectonemes and toroids for a region in F vs. n space. Nevertheless, recall that smaller values of α mean larger cooperativity and we would expect to see more than one nucleation site in experiment, which does not agree with the observations in (8).

- Increasing the value of the phenomenological parameter C_A and the exponential decay length λ in the DNA-DNA interactions Eq.15 in the main text, makes both collapsed states ($S + P$ and T) become energetically more favorable with respect to the straight configuration. Consequently as C_A and λ increase the value of $F_{critical}$ (transition force between states) increases as function of n.

We conclude that for large number of turns $n > n_{min}$ it is likely that the DNA state corresponds to a supercoiled configuration.

S.4.1 Energy source contributions

In Fig. S5 we show the relative dominance of each energetic source for the toroidal configuration including twist. Recall that the toroids energy is independent of the applied force F. The major energetic contributions correspond to surface energy and the DNA-DNA interactions. Bending energy is approximately constant as a function of the number of turns, while both the surface and twist energetic contributions increase as a function of the number of turns. In the case of the supercoiled-straight configurations, the energy is a function of both the force and the applied number of turns. For a given force F, the energy increases linearly with n, where l_p (length of the helical region) is the only variable as a function of n. In Fig. S6 we plot the specific energy contributions in the supercoiled-straight configuration as a function of F.

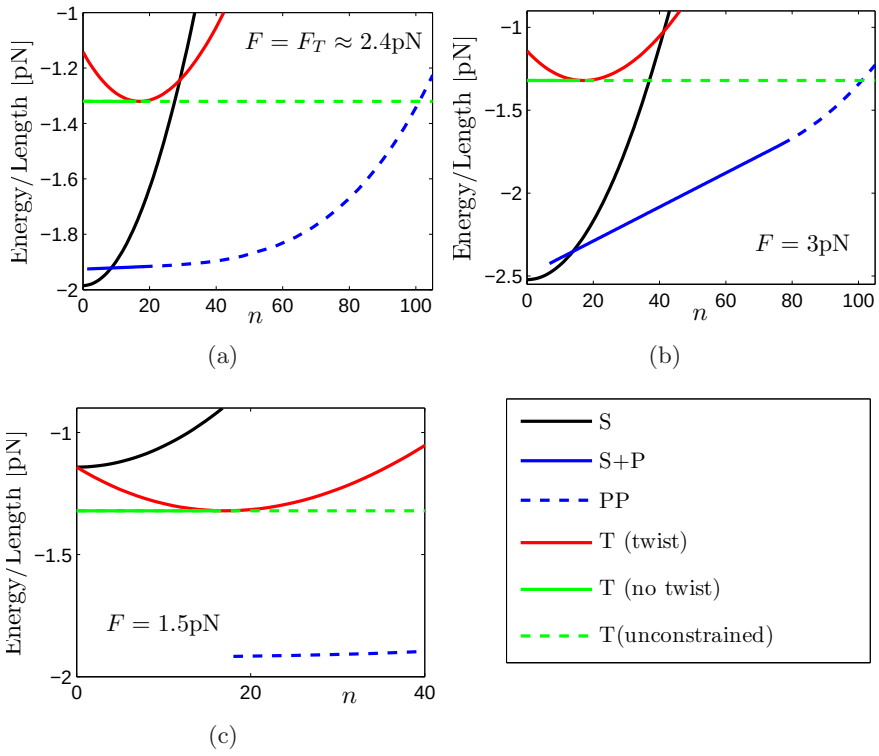

Figure S3: Energy density of competing structures as a function of the number of turns n for surface tension parameter $\alpha = 0.013$. The parameters used correspond to the theoretical solution for the description of Besteman et al. experiments in spermine in Fig. 2 in the main text. The black solid line corresponds to the straight configuration, the blue solid line to the straight + supercoiled coexistence, the blue dashed line correspond to the pure plectonemic phase, the red solid line correspond to toroids with twist and the green solid line correspond to toroids with no twist. Notice that the solution for toroids with no twist is only valid up to the point where the applied number of turns n is smaller than or equal to the toroid winding number N_g^o. The point where $n = N_g^o$ corresponds to the intersection of the red line and the green solid line. We have also plotted the energy density for torsionally unconstrained toroids depicted by the green dashed line. We point out that the torsionally unconstrained toroids which carry no twist are not a realistic solution for this problem. The link constraint on the DNA molecule must be taken into account otherwise toroids (unconstrained) would become energetically more favorable than supercoiled structures as n increases (green dashed line crosses the blue dashed line). The value of $n_{critical}$ (transition $S \rightarrow S + P$)is given by the intersection of the black solid line and blue solid line, the value of n_{pp} (transition $S + P \rightarrow PP$) is given by the intersection of the blue solid line with the blue dashed line. We have plotted the energy density for three representative forces F: (a) $F = F_T \approx 2.4$pN, supercoils are the favorable state for $n \geq n_{critical}$; (b) $F = 3\text{pN} > F_T$, for larger forces the intersection between the black solid line and blue line moves toward larger values of $n_{critical}$; (c) $F = 1.5\text{pN} < F_T$, there is no solution for the coexistence of straight + supercoiled, toroids are the preferred state up to n_{pp} which is the point were the PP solution starts.

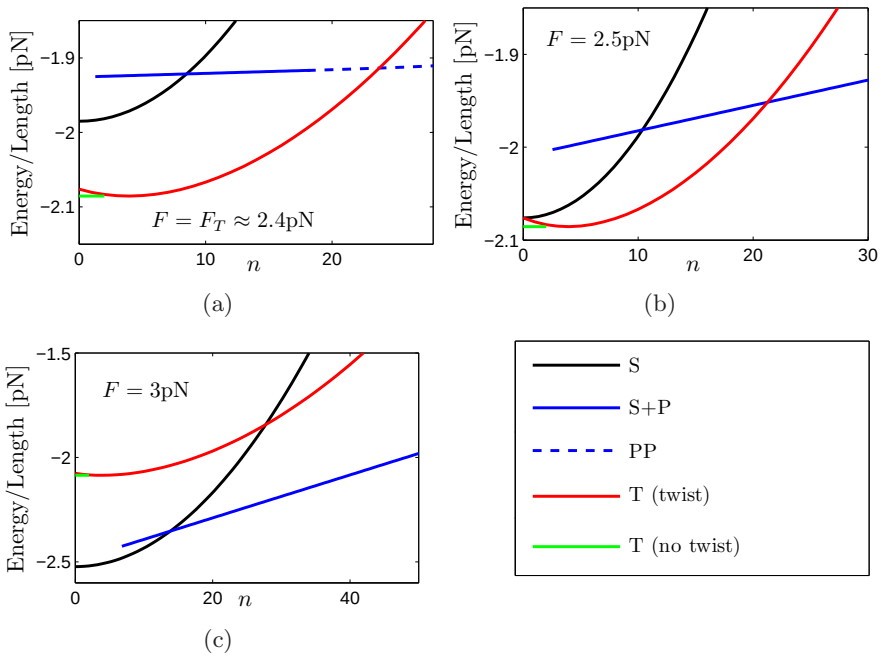

Figure S4: Energy density of competing structures as a function of the number of turns n for surface tension parameter $\alpha = 0.0003$. The rest of the parameters are the same as in Fig 2 in the main text. Lines represent the same energy densities as in Fig. S3, but here we do not present the solution for torsionally unconstrained toroids. Changing the value of α changes the preferred state of the DNA molecule as a function of the applied force F. Again we plot the energy density of the competing structures for three representative forces F: (a) $F = F_T \approx 2.4$pN, toroids are the preferred state up the intersection point of the blue dashed line and red solid line; (b) as the force increases $F = 2.5\text{pN} < F_T$, both the S and $S+P$ decrease its energy density, and at $n = 0$ the S and T(twist) have the same energy; (c) as the force further increases $F = 3\text{pN} > F_T$, the S configuration becomes the preferred state up to $n_{critical}$ and supercoils are the favorable state for $n \geq n_{critical}$.

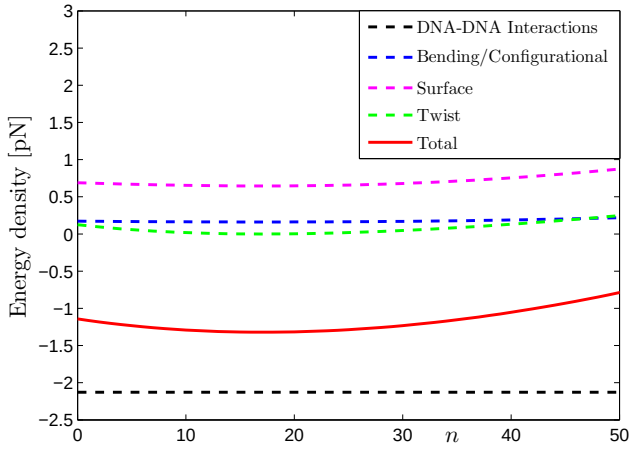

Figure S5: Energetic contribution in the toroidal configuration including twist. We use the same parameters as in Fig. 2 in the main text.

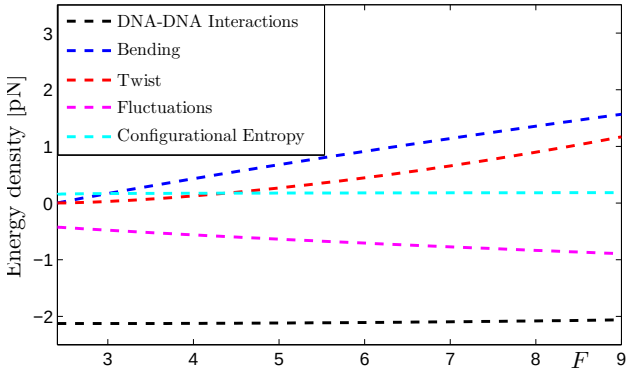

Figure S6: Energetic contributions in the supercoiled-straight configuration. We use the same parameters as in Fig. 2 in the main text.

Supporting References

1. Forth, S., C. Deufel, M. Y. Sheinin, B. Daniels, J. P. Sethna, and D. Wang, 2008. Abrupt buckling transition observed during the plectoneme formation of individual DNA molecules. *Phys. Rev. Lett.* 100(14):148301.

2. Brutzer, H., N. Luzzietti, D. Klaue, and R. Seidel, 2010. Energetics at the DNA Supercoiling Transition. *Biophys. J.* 98(7):1267–1276.

3. Mosconi, F., J. Allemand, D. Bensimon, and V. Croquette, 2009. Measurement of the Torque on a Single Stretched and Twisted DNA using Magnetic Tweezers. *Phys. Rev. Lett.* 102(7):078301.

4. Moroz, J., and P. Nelson, 1998. Entropic elasticity of twist-storing polymers. *Macromolecules* 31(18):6333–6347.

5. Murayama, Y., Y. Sakamaki, and M. Sano, 2003. Elastic response of single DNA molecules exhibits a reentrant collapsing transition. *Phys. Rev. Lett.* 90:018102.

6. Fu, W., X. Wang, X. Zhang, S. Ran, J. Yan, and M. Li, 2006. Compaction Dynamics of Single DNA Molecules under Tension. *J. Am. Chem. Soc.* 128:15040–15041.

7. Fu, W., H. Chen, M. Li, and J. Yan, 2010. Kinetics of Single DNA Compaction by Hexaamine Cobalt Chloride. *J. Comput. Theor. Nanosci.* 7:213–217.

8. van den Broek, B., M. Noom, J. van Mameren, C. Battle, F. MacKintosh, and G. Wuite, 2010. Visualizing the Formation and Collapse of DNA Toroids. *Biophys. J.* 98:1902–1910.

9. Besteman, K., S. Hage, N. Dekker, and S. Lemay, 2007. Role of Tension and Twist in Single-Molecule DNA Condensation. *Phys. Rev. Lett.* 98(5):058103.

10. Brewer, L., 2010. Deciphering the structure of DNA toroids. *Intgr. Biol.* pusblished online doi:10.1039/c0ib00128g.

11. Conwell, C., I. Vilffan, and N. Hud, 2003. Controlling the size of nanoscale toroidal DNA condensates with static curvature and ionic strength. *Proc. Natl. Acad. Sci.* 100:9296–9301.

12. Kúlic, I. M., H. Mohrbach, R. Thaokar, and H. Schiessel, 2007. Equation of state of looped DNA. *Phys. Rev. E.* 75(1):011913.

13. Strick, T., J. Allemand, V. Croquette, and D. Bensimon, 2000. Twisting and stretching single DNA molecules. *Prog. Biophys. Mol. Biol.* 74(1-2):115–140.

14. Hud, N., K. Downing, and R. Balhorn, 1995. A constant radius of curvature model for the organization of DNA in toroidal condensates. *Proc. Natl. Acad. Sci.* 92:3581–3585.

15. Shen, M., K. Downing, R. Balhorn, and N. Hud, 2000. Nucleation of DNA condensation by static loops: Formation of DNA toroids with reduced dimensions. *J. Am. Chem. Soc.* 122:4833–4834.

16. Battle, C., B. van der Broek, M. Noom, J. van Mameren, G. Wuite, and F. MacKintosh, 2009. Unraveling DNA tori under tension. *Phys. Rev. E.* 80:031917.

17. Park, S., D. Harries, and M. Gelbart, 1998. Topological Defects and the Optimum Size of DNA Condensates. *Biophys. J.* 75:714–720.

18. Cherstvy, A., 2005. Structure of DNA toroids and electrostatic attraction of DNA duplexes. *J. Phys. Condens. Matter.* 17:1363.

19. Ubbink, J., and T. Odijk, 1996. Deformation of toroidal DNA condensates under surface stress. *Europhys. Lett.* 33(5):353–358.

20. Ubbink, J., and T. Odijk, 1995. Polymer- and Salt-Induced toroids of Hegaxonal DNA. *Biophys. J.* 68:54–61.